

# Imposition of essential boundary conditions by displacement constraint equations in meshless methods

Xiong Zhang<sup>\*,†</sup>, Xin Liu, Ming-Wan Lu and Yong Chen

*Department of Engineering Mechanics, Tsinghua University, Beijing 100084, People's Republic of China*

## SUMMARY

One of major difficulties in the implementation of meshless methods is the imposition of essential boundary conditions as the approximations do not pass through the nodal parameter values. As a consequence, the imposition of essential boundary conditions in meshless methods is quite awkward. In this paper, a displacement constraint equations method (DCEM) is proposed for the imposition of the essential boundary conditions, in which the essential boundary conditions is treated as a constraint to the discrete equations obtained from the Galerkin methods. Instead of using the methods of Lagrange multipliers and the penalty method, a procedure is proposed in which unknowns are partitioned into two subvectors, one consisting of unknowns on boundary  $\Gamma_u$ , and one consisting of the remaining unknowns. A simplified displacement constraint equations method (SDCEM) is also proposed, which results in a efficient scheme with sufficient accuracy for the imposition of the essential boundary conditions in meshless methods. The present method results in a symmetric, positive and banded stiffness matrix. Numerical results show that the accuracy of the present method is higher than that of the modified variational principles. The present method is a exact method for imposing essential boundary conditions in meshless methods, and can be used in Galerkin-based meshless method, such as element-free Galerkin methods, reproducing kernel particle method, meshless local Petrov–Galerkin method. Copyright © 2001 John Wiley & Sons, Ltd.

KEY WORDS: meshless method; essential boundary condition; element-free Galerkin method

## 1. INTRODUCTION

During the past 30 years, the finite element (FE) method has been very successful in many research and engineering fields. However, the lack of robust and efficient 3D mesh generators makes the solution of 3D problems a difficult task. Furthermore, mesh-based methods are also not well suited to the problems associated with extremely large deformation and problems associated with frequent remeshing. Although several strategies have been developed to maintain a reasonable mesh shape, such as the arbitrary Lagrangian–Eularian (ALE) method, extra

\*Correspondence to: Xiong Zhang, Department of Engineering Mechanics, Tsinghua University, Beijing 100084, People's Republic of China

†E-mail: xzhang@tsinghua.edu.cn

Contract/grant sponsor: National Natural Science Foundation of China; contract/grant number: 19772024

computational effort and difficulties are also introduced. In the simulation of failure processes, frequent remeshing is required to model the propagation of cracks with arbitrary and complex paths so that the computational effort required is very significant.

To avoid these drawbacks of the FE, considerable effort has been devoted during recent years to the development of the so-called meshless method, and about 10 different meshless methods have been developed, such as the smoothed particle hydrodynamics (SPH) [1], the diffuse element (DE) method [2], the element-free Galerkin (EFG) method [3], the partition of unity finite element (PUFE) [4], the reproducing kernel particle (RKP) method [5], the finite point (FP) method [6], the hp clouds method [7, 8], the meshless local Petrov–Galerkin (MLPG) method [9], and several others. Based on the EFG, a meshless method has been proposed for discontinuum [10], such as jointed rock masses, in which rock blocks are modelled by EFG while joints are modelled by interfaces. The displacement fields are discontinuous across rock blocks.

One of the major difficulties in the implementation of meshless methods is the noninterpolatory character of the approximation, that is, the approximation does not pass through the nodal parameter values. As a consequence, the imposition of essential boundary conditions is quite awkward and several different approaches have been developed:

- (1) Direct collocation method [11–13].
- (2) Lagrange multiplier approaches [3, 14].
- (3) Modified variational principles [11, 12].
- (4) Penalty methods [9, 10, 15].
- (5) Coupling to finite element [16, 17].
- (6) Admissible approximation approaches [18].
- (7) d'Alembert's principle [19].
- (8) Modified collocation method [15].
- (9) Discrete form of essential boundary conditions [20].

As mentioned in Reference [21], the disadvantage of the Lagrange multiplier approaches is that the discrete equations for a linear self-adjoint partial differential equations (PDE) are no longer positive definite nor banded; moreover, this method leads to an awkward structure for the linear algebraic equations for the discrete system, and increases the number of unknowns. The approach based on the modified variational principles results in banded equations, but the boundary conditions are not imposed as accurate as the method of Lagrange multipliers, and might bring unstable solutions [22]. The penalty methods are very simple to be implemented, but the penalty must be chosen appropriately.

In the coupled EFG/FE approach, elements are placed around the boundary of the domain so that the essential boundary conditions are applied to finite element nodes by standard methods. In admissible approximation approach, the essential boundary conditions are imposed by forcing the weight function to be zero on Dirichlet boundaries [18]. In Reference [20], the trial function is modified based on the weak form of the essential boundary conditions to satisfy the kinematic (essential) boundary conditions in the sense of weak form. Lu and Belytschko proved that the weak form of essential boundary conditions is identical to the method of Lagrange multipliers if the same shape functions are used for the Lagrange multipliers and the test and trial functions.

In the direct collocation method, the collocation condition,  $\hat{u}_i = \bar{u}$  on boundary  $\Gamma_u$ , is used, where  $\bar{u}$  are the prescribed nodal displacements on boundary  $\Gamma_u$ . However,  $\hat{u}$  is not the final

displacement vector at nodes in MLS. It contains the fictitious nodal values used to fit the displacement functions with the MLS approximation. Therefore, enforcement of  $\hat{u} = \bar{u}$  on  $\Gamma_u$  is not appropriate [15]. The modified collocation method [15] is shown to yield much more accurate results than the direct collocation methods, but the stiffness matrix obtained is unsymmetrical.

Günther and Liu [19] proposed a algorithm based on the d'Alembert's principle that can be used for general constraints both in meshless methods and finite elements. In their scheme,  $n$  differential equations and  $m$  constraints are replaced by  $n-m$  equations through choosing  $n-m$  generalized variables. Meanwhile, the Gram-Schmidt algorithm is used to determine the Jacobi matrix and to orthogonalize the constraints.

In this paper, a displacement constraint equations method is proposed for the imposition of the essential boundary conditions in meshless methods, in which the essential boundary conditions is treated as a displacement constraint to the discrete equations obtained from Galerkin methods. Unlike the procedure proposed in Reference [19], the unknown parameters are partitioned into two subvectors; one consisting of unknowns on boundary  $\Gamma_u$ , and one consisting of the remaining unknowns. All other matrices and vectors are also partitioned in the same way. The present procedure is a exact method, and results in a system with a reduced number of unknowns. Compared with Lagrange multipliers method and Penalty method, computational effort required is reduced and the accuracy of the solution is improved. A simplified approach is also proposed to further reduce the computational effort required. As a test, a cantilever beam, an infinite plate with hole, and a two-dimensional Poisson equation are analyzed in detail. The present approaches give more accurate results than the modified variational principles, and can be used in Galerkin-based meshless methods, such as EFG, RKP, and MLPG, etc.

## 2. GALERKIN METHOD

Two methods of discretization have been dominant in existing meshless methods [21]:

- (1) Collocation methods, which are used in SPH [1], hp-meshless cloud method [7] and FPM [6].
- (2) Galerkin methods or Petrov-Galerkin methods, which are used in EFG [3], hp clouds [8], PUFEM [4], RKPM [5], MLPG [9] and other methods.

In collocation methods, essential boundary conditions can be easily imposed so that only Galerkin methods and Petrov Galerkin methods are discussed in this paper.

As an example, we will consider the two-dimensional problem

$$\nabla \cdot \boldsymbol{\sigma} + \mathbf{f} = 0 \quad \text{in } \Omega \tag{1}$$

$$\mathbf{u} = \bar{\mathbf{u}} \quad \text{on } \Gamma_u \tag{2}$$

$$\boldsymbol{\sigma} \cdot \mathbf{n} = \bar{\mathbf{t}} \quad \text{on } \Gamma_t \tag{3}$$

where  $\mathbf{n}$  is the unit normal to the boundary  $\Gamma_t$ ,  $\boldsymbol{\sigma}$  is the stress tensor,  $\mathbf{u}$  the displacement field,  $\mathbf{f}$  the body force. In (1)–(3), the superposed bar denotes prescribed boundary values.

The weak form of (1) is given by

$$\int_{\Omega} \nabla_s \delta \mathbf{u} : \boldsymbol{\sigma} \, d\Omega - \int_{\Omega} \delta \mathbf{u} \cdot \mathbf{f} \, d\Omega - \int_{\Gamma_t} \delta \mathbf{u} \cdot \bar{\mathbf{t}} \, d\Gamma = 0 \quad (4)$$

where the test function  $\delta \mathbf{u}$  vanishes on  $\Gamma_u$ . In the above,  $\nabla_s \mathbf{u}$  is the symmetric part of  $\nabla \mathbf{u}$ . Meshless approximation function  $u^h(x)$  can be expressed as

$$u^h(x) = \sum_{I=1}^{n_p} N_I(x) u_I \quad (5)$$

where  $n_p$  is the total number of nodes in the domain of definition of the meshless approximation,  $u^h(x)$ , for the trial function  $u$  at  $x$ ,  $N_I(x)$  is the shape function of meshless approximation corresponding to node  $x_I$  evaluated at  $x$ , and  $u_I$  is the nodal value of  $u(x)$  at node  $x = x_I$ . Shape functions  $N_I(x)$  can be constructed by various approximation methods resulting in different meshless methods. Substituting (5) into (4) leads to the discrete equations

$$\mathbf{K}\mathbf{U} = \mathbf{F} \quad (6)$$

where

$$\mathbf{K} = \int_{\Omega} \mathbf{B}^T \mathbf{D} \mathbf{B} \, d\Omega \quad (7)$$

$$\mathbf{F} = \int_{\Omega} \mathbf{N}(x) \mathbf{f} \, d\Omega + \int_{\Gamma_t} \mathbf{N}(x) \bar{\mathbf{t}} \, d\Gamma \quad (8)$$

$$\mathbf{U} = [u_1 \ u_2 \ \cdots \ u_N]^T \quad (9)$$

and  $N$  is the total number of nodes in  $\Omega$ ,  $\Gamma_u$  and  $\Gamma_t$ . The discrete equations for other type of PDE are similar to (6), with the exception of different definition of coefficient matrices  $\mathbf{K}$  and  $\mathbf{F}$ .

### 3. ESSENTIAL BOUNDARY CONDITIONS

Because the approximations  $u^h(x)$  do not satisfy the finite-element-like Kronecker delta condition, the imposition of the essential boundary conditions (2) is quite awkward in meshless methods. Actually, the essential boundary condition (2) is a constraint to the weak form of PDE. Instead of using the method of Lagrange multipliers, a efficient and simple procedure is proposed in this paper to solve this constrained problem.

Let  $S_u$  be the set of nodes which are on  $\Gamma_u$ , and  $S$  the total set of nodes. Suppose there are  $n_u$  nodes in  $S_u$  and  $N$  nodes in  $S$ . Substituting the meshless approximation function (5) into the essential boundary condition (2) leads to

$$\mathbf{B}\mathbf{U} = \bar{\mathbf{U}} \quad (10)$$

where

$$\mathbf{B}_{iJ} = N_J(x_i) \quad (11)$$

$$\bar{\mathbf{U}}_i = \bar{u}(x_i), \quad i \in S_u, \ J \in S \quad (12)$$

Equation (6) must be solved under the constraint of (10). However, there are  $N$  unknowns and  $N + n_u$  equations in (6) and (10), so that they can not be solved directly. Based on d'Alembert's principles, Günther and Liu [19] proposed a scheme which can be used for general constraints. In their scheme, the linear constraint (10) was orthogonalized by using the Gram–Schmidt algorithm so that

$$\mathbf{B}\mathbf{B}^T = \mathbf{I} \quad (13)$$

where  $\mathbf{I}$  is the identity matrix. Again, the Gram–Schmidt algorithm was used to obtain an  $(N - n_u) \times N$  Jacobi matrix  $\mathbf{J}$  with

$$\mathbf{J}\mathbf{B}^T = 0 \quad (14)$$

$$\mathbf{J}\mathbf{J}^T = \mathbf{I} \quad (15)$$

The unknown vector  $\mathbf{U}$  can be written using generalized variables  $\mathbf{y}$  as

$$\mathbf{U} = \mathbf{J}^T\mathbf{y} + \mathbf{B}^T\bar{\mathbf{U}} \quad (16)$$

Substituting (16) into (6) and premultiplying by  $\mathbf{J}$  leads to

$$\tilde{\mathbf{K}}\mathbf{y} = \tilde{\mathbf{F}} \quad (17)$$

with

$$\tilde{\mathbf{K}} = \mathbf{J}\mathbf{K}\mathbf{J}^T$$

$$\tilde{\mathbf{F}} = \mathbf{J}(\mathbf{F} - \mathbf{K}\mathbf{B}^T\bar{\mathbf{U}})$$

Equation (17) is a system of  $(N - n_u) \times (N - n_u)$  linear algebraic equations.

In this paper, another simple and efficient scheme is proposed to solve this constrained problem. The nodes are so numbered that  $\mathbf{U}$  can be partitioned into two subvectors;  $\mathbf{U}_1$  consisting of unknowns in  $\Omega - \Gamma_u$ , and  $\mathbf{U}_2$  consisting of unknowns on  $\Gamma_u$ , that is

$$\mathbf{U} = [\mathbf{U}_1^T \quad \mathbf{U}_2^T]^T \quad (18)$$

where  $\mathbf{U}_1 \in R^{N-n_u}$ , and  $\mathbf{U}_2 \in R^{n_u}$ . Other matrices and vectors are also partitioned in the same way, so that

$$\mathbf{B} = [\mathbf{B}_1 \quad \mathbf{B}_2] \quad (19)$$

$$\mathbf{K} = \begin{bmatrix} \mathbf{K}_{11} & \mathbf{K}_{12} \\ \mathbf{K}_{21} & \mathbf{K}_{22} \end{bmatrix} \quad (20)$$

$$\mathbf{F} = [\mathbf{F}_1^T \quad \mathbf{F}_2^T]^T \quad (21)$$

where  $\mathbf{B}_2$  is a square matrix of order  $n_u$ , and  $\mathbf{K}_{11}$  a square matrix of order  $N - n_u$ . Subvector  $\mathbf{U}_2$  is obtained as the solution of (10), namely

$$\mathbf{U}_2 = \mathbf{B}_2^{-1}\bar{\mathbf{U}} - \mathbf{B}_2^{-1}\mathbf{B}_1\mathbf{U}_1 \quad (22)$$

Substituting (22) into (18) results in

$$\mathbf{U} = \hat{\mathbf{U}} + \mathbf{T}\mathbf{U}_1 \quad (23)$$

where

$$\hat{\mathbf{U}} = \begin{bmatrix} \mathbf{0} \\ \mathbf{B}_2^{-1}\hat{\mathbf{U}} \end{bmatrix}, \quad \mathbf{T} = \begin{bmatrix} \mathbf{I} \\ -\mathbf{B}_2^{-1}\mathbf{B}_1 \end{bmatrix} \quad (24)$$

Substituting (23) into (6), and premultiplying by  $\mathbf{T}^T$  leads to a system with  $N - n_u$  unknowns, namely

$$\bar{\mathbf{K}}\mathbf{U}_1 = \bar{\mathbf{F}} \quad (25)$$

where

$$\bar{\mathbf{K}} = \mathbf{T}^T\mathbf{K}\mathbf{T} \quad (26)$$

$$\bar{\mathbf{F}} = \mathbf{T}^T(\mathbf{F} - \mathbf{K}\hat{\mathbf{U}}) \quad (27)$$

In (25), matrix  $\bar{\mathbf{K}}$  is symmetric and also positive definite if sufficient constraints are provided. It will be shown that  $\bar{\mathbf{K}}$  is also banded. After  $\mathbf{U}_1$  is obtained from (25),  $\mathbf{U}_2$  can be obtained from (22). Because the order of matrix  $\mathbf{B}_2$  is very low, the computational effort required for the calculation of  $\bar{\mathbf{K}}$  and  $\bar{\mathbf{F}}$  in (26) and (27) is not significant, so that the present scheme is efficient. Meanwhile, the present scheme is an exact scheme for the imposition of essential boundary condition in meshless methods.

Comparing (25) and (17), one can deduce that the present method is different from that proposed in Reference [19]. Although the order of (25) is identical to that of (17), the matrices  $\bar{\mathbf{K}}$  and  $\bar{\mathbf{F}}$  in (25) are different from  $\bar{\mathbf{K}}$  and  $\bar{\mathbf{F}}$  in (17). Compared with (17), the present method is more efficient because only factorization of a  $n_u \times n_u$  ( $n_u \ll N$ ) matrix,  $\mathbf{B}_2$ , is required to obtain the transformation matrix  $\mathbf{T}$ . In the next section, a simplified approach is developed so that  $\mathbf{B}_2$  become a diagonal matrix. Consequently,  $\bar{\mathbf{K}}$  and  $\bar{\mathbf{F}}$  are very easy to be calculated.

Actually, the imposition of essential boundary conditions in the finite element method is a special case of the present method. In the finite element method, matrix  $\mathbf{B}$  is given by

$$\mathbf{B} = [\mathbf{0} \quad \mathbf{I}] \quad (28)$$

Substituting (28) into (26) and (27) leads to

$$\bar{\mathbf{K}} = \mathbf{K}_{11} \quad (29)$$

$$\bar{\mathbf{F}} = \mathbf{F}_1 - \mathbf{K}_{12}\hat{\mathbf{U}} \quad (30)$$

This is just the standard formulation for the imposition of essential boundary conditions in the finite element method.

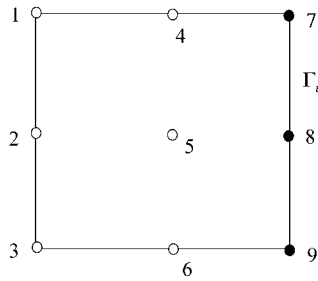


Figure 1. A simple example.

#### 4. SIMPLIFIED APPROACH

To develop a simplified scheme, Equations (26) and (27) can be rewritten as

$$\bar{\mathbf{K}} = \mathbf{K}_{11} - (\mathbf{B}_2^{-1}\mathbf{B}_1)^T \mathbf{K}_{21} - \mathbf{K}_{12}(\mathbf{B}_2^{-1}\mathbf{B}_1) + (\mathbf{B}_2^{-1}\mathbf{B}_1)^T \mathbf{K}_{22}(\mathbf{B}_2^{-1}\mathbf{B}_1) \quad (31)$$

$$\bar{\mathbf{F}} = \mathbf{F}_1 - (\mathbf{B}_2^{-1}\mathbf{B}_1)^T \mathbf{F}_2 - [\mathbf{K}_{12} - (\mathbf{B}_2^{-1}\mathbf{B}_1)^T \mathbf{K}_{22}] \mathbf{B}_2^{-1} \bar{\mathbf{U}} \quad (32)$$

For convenience, the problem shown in Figure 1 is considered, in which nodes 7–9 are on boundary  $\Gamma_u$ . Assume that nodes 4 and 8 are located in the support of node 7, nodes 5, 7 and 9 are located in the support of node 8, and nodes 6 and 8 are located in the support of node 9. In this particular case, matrix  $\mathbf{B}$  is a  $3 \times 9$  matrix, i.e.

$$\mathbf{B} = \begin{bmatrix} 0 & 0 & 0 & * & 0 & 0 & * & * & 0 \\ 0 & 0 & 0 & 0 & * & 0 & * & * & * \\ 0 & 0 & 0 & 0 & 0 & * & 0 & * & * \end{bmatrix} \quad (33)$$

and  $\mathbf{B}_2^{-1}$  is a full matrix. In (33), asterisk represents a non-zero entry. The matrix  $\mathbf{B}_2^{-1}\mathbf{B}_1$  can be expressed as

$$\mathbf{B}_2^{-1}\mathbf{B}_1 = [[0]_{3 \times 3} \quad [*]_{3 \times 3}] \quad (34)$$

where  $[*]_{3 \times 3}$  represents a  $3 \times 3$  full real matrix, and  $[0]_{3 \times 3}$  a  $3 \times 3$  zero matrix. The matrix  $\mathbf{K}_{21}$  is of the same form as  $\mathbf{B}_1$ , i.e.

$$\mathbf{K}_{21} = \begin{bmatrix} 0 & 0 & 0 & * & 0 & 0 \\ 0 & 0 & 0 & 0 & * & 0 \\ 0 & 0 & 0 & 0 & 0 & * \end{bmatrix} \quad (35)$$

The second and third terms in (31) are given by

$$\begin{bmatrix} [0]_{3 \times 3} & [0]_{3 \times 3} \\ [0]_{3 \times 3} & [*]_{3 \times 3} \end{bmatrix} \quad (36)$$

Equation (36) shows that nodes 4–6 are fully coupled in  $\bar{\mathbf{K}}$ , disregarding whether they are coupled in  $\mathbf{K}_{11}$ . This character also holds for the last term in (31). As a consequence, although  $\bar{\mathbf{K}}$  is a banded matrix, but its band widths are different from those of  $\mathbf{K}_{11}$ . This is due to the fullness of matrix  $\mathbf{B}_2^{-1}$ .

From physical points of view, because node 8 is located in the support of node 7, all nodes in the support of node 8 will be coupled with nodes in the support of node 7. For the same reason, all nodes in the support of node 9 are also coupled with nodes in the supports of nodes 7 and 8. Consequently, nodes 4–6 will be fully coupled, disregarding whether node 6 is in the support of node 4. Keeping this point in mind, the band widths of matrix  $\bar{\mathbf{K}}$  can be easily determined prior to the calculation of its elements. Usually, the support of nodes on boundary  $\Gamma_u$  is only a small part of  $\Omega$ , so that the band widths of  $\bar{\mathbf{K}}$  are very close to those of  $\mathbf{K}_{11}$ .

In hp-meshless cloud method [7], a relatively simple and effective selection algorithm are adopted to select nodes used to construct the interpolation functions. In this algorithm, not all nodes in the support of a node are used in the construction of the interpolation functions. Based on this consideration, it is reasonable to exclude other boundary nodes from the support of a boundary node when assemble the boundary condition matrix  $\mathbf{B}$  in (10). For instance, nodes 7 and 9 will be excluded from the support of node 8. Consequently, matrix  $\mathbf{B}_2$  is a diagonal matrix, so that the band widths of matrix  $\bar{\mathbf{K}}$  are the exactly same as those of matrix  $\mathbf{K}_{11}$ . Meanwhile, matrices  $\bar{\mathbf{K}}$  and  $\bar{\mathbf{F}}$  in (25) can be obtained efficiently. Numerical studies presented in Section 5 show that this simplified method gives almost the same results as those obtained by the method without the simplification.

The present method can be easily implemented in an existing Galerkin based meshless code. Note that  $\mathbf{K}_{11}$  depends on nodes in  $\Omega - \Gamma_u$ , and is independent of nodes on boundary  $\Gamma_u$ . Only  $\mathbf{K}_{11}$ ,  $\mathbf{K}_{21}$  and  $\mathbf{B}_1$  are needed to be allocated, and matrix  $\bar{\mathbf{K}}$  can share storage with  $\mathbf{K}_{11}$ .

## 5. NUMERICAL EXAMPLES

The present method is implemented in the computer code developed in References [10, 23], which are based on EFG. The exponential weight function

$$w_I(d_I) = \begin{cases} \frac{e^{-(d_I/c)^2} - e^{-(d_{ml}/c)^2}}{1 - e^{-(d_{ml}/c)^2}} & \text{if } d_I < d_{ml} \\ 0 & \text{if } d_I \geq d_{ml} \end{cases} \quad (37)$$

proposed in Reference [3] is used. In this paper, the domain of definition of the MLS approximation for the trial function at a quadrature point is a circle, whose radius,  $d_{ml}$ , is chosen automatically to ensure that the total number of nodes in the circle equals  $3m$ , where  $m$  is the number of monomials included in the basis of the moving least square interpolant and is set to 6 (quadratic basis) in the numerical examples presented in this section.

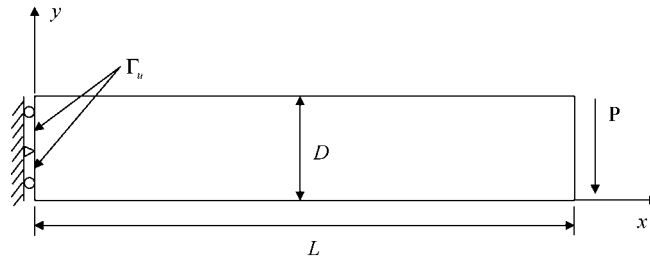


Figure 2. Cantilever beam.

For accuracy studies, the  $L_2$  relative error norm in displacement and stress are calculated by

$$\|e_2^u\| = \frac{\left[ \int_{\Omega} (u^h(x) - u^{\text{exact}}(x))^T (u^h(x) - u^{\text{exact}}(x)) \, d\Omega \right]^{1/2}}{\left[ \int_{\Omega} (u^{\text{exact}}(x))^T u^{\text{exact}}(x) \, d\Omega \right]^{1/2}} \quad (38)$$

$$\|e_2^\sigma\| = \frac{\left[ \int_{\Omega} (\sigma^h(x) - \sigma^{\text{exact}}(x))^T (\sigma^h(x) - \sigma^{\text{exact}}(x)) \, d\Omega \right]^{1/2}}{\left[ \int_{\Omega} (\sigma^{\text{exact}}(x))^T \sigma^{\text{exact}}(x) \, d\Omega \right]^{1/2}} \quad (39)$$

respectively. In (38) and (39),  $u^{\text{exact}}(x)$  and  $\sigma^{\text{exact}}(x)$  are the exact solution of displacement and stress at  $x$ ,  $u^h(x)$  and  $\sigma^h(x)$  are the approximation of displacement and stress at  $x$ , respectively.

### 5.1. Cantilever beam

The exact solution for cantilever beam subjected to end load as shown in Figure 2 is given by Timoshenko and Goodier [24] as

$$u_x = -\frac{P}{6EI} \left( y - \frac{D}{2} \right) [(6L - 3x)x + (2 + \nu)(y^2 - Dy)] \quad (40)$$

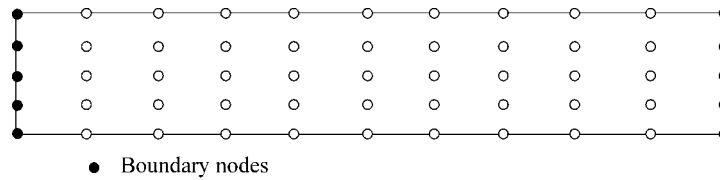
$$u_y = \frac{P}{6EI} \left[ 3\nu \left( y - \frac{1}{2}D \right)^2 (L - x) + \frac{1}{4}(4 + 5\nu)D^2x + (3L - x)x^2 \right] \quad (41)$$

where  $E$  is the elastic modulus,  $\nu$  is the Poisson's ratio, and  $I$  is the moment of inertia which is given by  $D^3/12$  for a beam with rectangular cross-section and unit thickness. The stresses are

$$\sigma_{xx} = -\frac{P}{I}(L - x) \left( y - \frac{1}{2}D \right) \quad (42)$$

$$\sigma_{yy} = 0 \quad (43)$$

$$\sigma_{xy} = -\frac{Py}{2I}(y - D) \quad (44)$$

Figure 3.  $9 \times 5$  regular data points.Table I.  $L_2$  relative error norm in displacement (per cent).

$d_{ml}/c$	Penalty method	Constraint equations method	Simplified method
3.0	1.44	1.43	1.42
3.5	1.06	1.06	1.09
4.0	0.85	0.85	0.87

Table II.  $L_2$  relative error norm in stress (per cent).

$d_{ml}/c$	Penalty method	Constraint equations method	Simplified method
3.0	8.54	8.53	8.73
3.5	8.28	8.28	8.52
4.0	8.33	8.33	8.46

This problem is solved with dimensionless parameters  $E = 1.0 \times 10^3$ ,  $\nu = \frac{1}{3}$ ,  $P = 6$ ,  $D = 2$  and  $L = 12$ . The nodal arrangements used in the analysis as well as the nodes used to enforce boundary conditions are shown in Figure 3.  $10 \times 6$  cell structure is used for quadrature, with  $4 \times 4$  Gauss quadrature in each cell. Numerical results are strongly dependent on the choice of parameter  $c$  used in the MLS approximation. Errors in displacement and stress are given in Tables I and II for different value of  $d_{ml}/c$ . This numerical study also shows that the simplified method is accurate and efficient.

### 5.2. An infinite plate with hole

An infinite plate with a central circular hole is subjected to a unidirectional tensile load of 1.0 in the  $x$  direction. Due to symmetry, only the upper-right quadrant of the plate is modelled. Elastic modulus  $E$  and Poisson's ratio  $\nu$  are assumed to be  $1.0 \times 10^3$  and 0.3, respectively. Symmetry conditions are imposed on the left and bottom edges, and the inner boundary at  $a = 1$  is traction-free. The exact solution for the stresses is

$$\sigma_x(x, y) = 1 - \frac{a^2}{r^2} \left( \frac{3}{2} \cos 2\theta + \cos 4\theta \right) + \frac{3a^4}{2r^4} \cos 4\theta \quad (45)$$

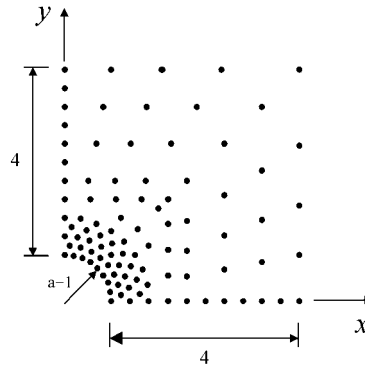


Figure 4. Data points.

Table III.  $L_2$  relative error norm in stress for the infinite plate with hole (per cent).

$d_{ml}/c$	Penalty method	Constraint equations method	Simplified method
2.5	9.68	9.68	9.67
3.0	10.78	10.78	10.79
3.5	10.74	10.74	10.76

$$\sigma_y(x, y) = -\frac{a^2}{r^2} \left( \frac{1}{2} \cos 2\theta - \cos 4\theta \right) - \frac{3a^4}{2r^4} \cos 4\theta \tag{46}$$

$$\tau_{xy}(x, y) = -\frac{a^2}{r^2} \left( \frac{1}{2} \sin 2\theta + \sin 4\theta \right) + \frac{3a^4}{2r^4} \sin 4\theta \tag{47}$$

where  $(r, \theta)$  are the usual polar coordinates and  $\theta$  is measured from the positive  $x$  axis counterclockwise. Traction boundary conditions given by the exact solutions (45)–(47) are imposed on the right ( $x = 5$ ) and top ( $y = 5$ ) edges. There are 98 data points and 40 cells in the analysis, with  $4 \times 4$  Gauss quadrature in each cell. Figure 4 shows the nodal arrangement used in the analysis, and  $L_2$  relative norm in stress are listed in Table III for different value of  $d_{ml}/c$ .

### 5.3. Poisson equation

Consider Poisson equation,

$$\begin{aligned} \nabla^2 u &= -2(x + y - x^2 - y^2) \quad \text{in } \Omega = [0, 1] \times [0, 1] \\ u &= 0 \quad \text{on } \partial\Omega \end{aligned}$$

whose analytical solution is given by

$$u(x, y) = (x - x^2)(y - y^2)$$

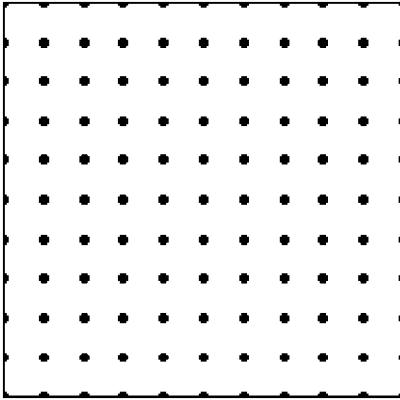


Figure 5. Regular nodal arrangement with 121 nodes.

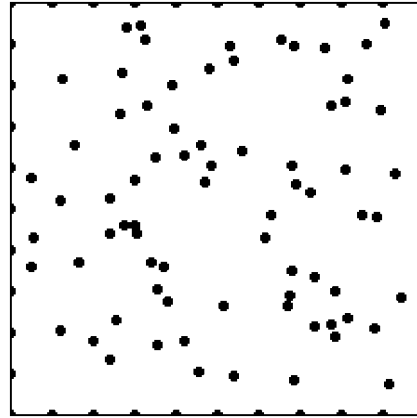


Figure 6. Irregular nodal arrangement with 114 nodes.

Table IV.  $L_2$  relative error norm for regular nodal arrangement (%).

$c/d_{ml}$	Constraint equation method	Simplified method	Modified variational principles
0.30	0.35	0.39	0.48
0.45	2.07	2.08	2.27

Table V.  $L_2$  relative error norm for irregular nodal arrangement (per cent).

$c/d_{ml}$	Constraint equations method	Simplified method	Modified variational principles
0.30	1.17	1.18	4.07
0.45	3.47	3.35	4.56

This problem is analyzed by using a regular and an irregular nodal arrangement, as shown in Figures 5 and 6. Numerical results are compared with those obtained by the modified variational principles with different value of  $c$  in Tables IV and V.

## 6. CONCLUDING REMARKS

In this paper, the essential boundary conditions are imposed by constraint equations method. A efficient and accurate scheme is proposed to solve this constrained problem, which reduce a system of  $N \times N$  algebraic equations (6) and  $n_u$  constraints into a system of  $(N - n_u) \times (N - n_u)$  algebraic equations. The present method is a exact method for imposing the essential boundary

conditions in meshless methods, and it is superior to the method of Lagrange multipliers, the modified variational principles and the penalty method. A simplified method is also proposed in this paper. For most cases, the simplified method gives almost the same results as those given by the method without simplification, while it simplifies the calculation significantly. Therefore the simplified method is recommended.

## ACKNOWLEDGEMENTS

This work was supported by the National Natural Science Foundation of China under grant number 19772024.

## REFERENCES

1. Gingold RA, Moraghan JJ. Smoothed particle hydrodynamics: theory and applications to non-spherical stars. *Monthly Notices of the Astronomical Society* 1977; **181**:375–389.
2. Nayroles B, Touzot G, Villon P. Generalizing the FEM: diffuse approximation and diffuse elements. *Computational Mechanics* 1992; **10**:307–318.
3. Belytschko T, Lu Y, Gu L. Element free Galerkin methods. *International Journal for Numerical Methods in Engineering* 1994; **37**:229–256.
4. Melenk JM, Babuška I. The partition of unity finite element method: basic theory and applications. *Computer Methods in Applied Mechanics and Engineering* 1996; **139**:289–314.
5. Liu WK, Jun S, Zhang YF. Reproducing kernel particle methods. *International Journal for Numerical Methods in Fluids* 1995; **20**:1081–1106.
6. Oñate E, Idelsohn S, Zienkiewicz OC, Taylor RL. A finite point method in computational mechanics. Applications to convective transport and fluid flow. *International Journal for Numerical Methods in Engineering* 1990; **39**:3839–3866.
7. Liszka TJ, Duarte CAM, Tworzydło WW. hp-meshless cloud method. *Computer Methods in Applied Mechanics and Engineering* 1996; **139**:263–288.
8. Duarte CA, Oden JT. An h-p adaptive method using clouds. *Computer Methods in Applied Mechanics and Engineering* 1996; **139**:237–262.
9. Atluri SN, Zhu T-L. A new meshless local Petrov–Galerkin (MLPG) approach. In *Modelling and Simulation Based Engineering*, vol. 1, Atluri SN, O’Donoghue PE (eds). Tech Science Press: Palmdale, CA, 1998; 2–10.
10. Zhang X, Lu M-W, Wegner JL. A meshless model for jointed rock structures. *International Journal for Numerical Methods in Engineering* 2000; **47**:1649–1661.
11. Lu YY, Belytschko T, Gu L. A new implementation of the element free Galerkin method. *Computer Methods in Applied Mechanics and Engineering* 1994; **113**:397–414.
12. Mukherjee YX, Mukherjee S. On boundary conditions in the element free Galerkin method. *Computational Mechanics* 1997; **19**:267–270.
13. Belytschko T, Tabbara M. Dynamic fracture using element-free Galerkin methods. *International Journal for Numerical Methods in Engineering* 1996; **39**:923–938.
14. Krysl P, Belytschko T. Analysis of thin plates by the element-free Galerkin methods. *Computational Mechanics* 1995; **17**:26–35.
15. Zhu T, Atluri SN. Modified collocation method and a penalty formulation for enforcing the essential boundary conditions in the element free Galerkin method. *Computational Mechanics* 1998; **21**:211–222.
16. Krongauz Y, Belytschko T. Enforcement of essential boundary conditions in meshless approximations using finite elements. *Computer Methods in Applied Mechanics and Engineering* 1996; **131**:133–145.
17. Hegen D. Element-free Galerkin methods in combination with finite element approaches. *Computer Methods in Applied Mechanics and Engineering* 1996; **135**:143–166.
18. Gosz J, Liu WK. Admissible approximations for essential boundary conditions in the reproducing kernel particle method. *Computational Mechanics* 1996; **19**:120–135.
19. Günther FC, Liu WK. Implementation of boundary conditions for meshless methods. *Computer Methods in Applied Mechanics and Engineering* 1998; **163**:205–230.
20. Lu YY, Belytschko T, Tabbara M. Element-free Galerkin method for wave propagation and dynamic fracture. *Computer Methods in Applied Mechanics and Engineering* 1995; **126**:131–153.

21. Belytschko T, Krongauz Y, Organ D, Fleming M. Meshless methods: an overview and recent developments. *Computer Methods in Applied Mechanics and Engineering* 1996; **119**:3–47.
22. Xue WM. Existence, uniqueness, and stability conditions for general finite element methods in linear elasticity. *PhD Thesis*, Georgia Institute of Technology, 1984.
23. Liu X. Study on meshless numerical methods. *PhD Dissertation*, Nanjing University of Aeronautics and Astronautics, People's Republic of China, July 1998.
24. Timoshenko SP, Goodier JN. *Theory of Elasticity* (3rd ed). McGraw-Hill: New York, 1987.
25. Chu YA, Moran B. A computational model for nucleation of solid-solid phase transformations. *Modeling Simulations Materials Science and Engineering* 1995; **3**:455–471.
26. Bathe KJ. *Finite Element Procedures in Engineering Analysis*. Prentice-Hall, Inc: Englewood Cliffs, NJ, 1982.